

Accepted Manuscript

Design and Synthesis of Donepezil Analogues as Dual AChE and BACE-1 inhibitors

Moustafa T. Gabr, Mohammed S. Abdel-Raziq

PII: S0045-2068(18)30412-7
DOI: <https://doi.org/10.1016/j.bioorg.2018.06.031>
Reference: YBIOO 2411

To appear in: *Bioorganic Chemistry*

Received Date: 27 April 2018
Revised Date: 20 June 2018
Accepted Date: 23 June 2018

Please cite this article as: M.T. Gabr, M.S. Abdel-Raziq, Design and Synthesis of Donepezil Analogues as Dual AChE and BACE-1 inhibitors, *Bioorganic Chemistry* (2018), doi: <https://doi.org/10.1016/j.bioorg.2018.06.031>

This is a PDF file of an unedited manuscript that has been accepted for publication. As a service to our customers we are providing this early version of the manuscript. The manuscript will undergo copyediting, typesetting, and review of the resulting proof before it is published in its final form. Please note that during the production process errors may be discovered which could affect the content, and all legal disclaimers that apply to the journal pertain.



Design and Synthesis of Donepezil Analogues as Dual AChE and BACE-1 inhibitors

Moustafa T. Gabr^{a,b*} and Mohammed S. Abdel-Raziq^{c,d}

^aDepartment of Medicinal Chemistry, Faculty of Pharmacy, Mansoura University, Mansoura 35516, Egypt

^bDepartment of Chemistry, University of Iowa, Iowa City, Iowa 52242, USA

^cFaculty of Pharmacy, Mansoura University, Mansoura 35516, Egypt

^dSchool of Chemistry and Molecular Biosciences, University of Queensland, St Lucia 4072, Queensland, Australia

*Corresponding author: Tel.: +1 3193599500; E-mail address: gabr2003@gmail.com

Abstract: Multi-target-directed ligands (MTDLs) centered on β -secretase 1 (BACE-1) inhibition are emerging as innovative therapeutics in addressing the complexity of neurodegenerative diseases. A new series of donepezil analogues was designed, synthesized and evaluated as MTDLs against neurodegenerative diseases. Profiling of donepezil, a potent acetylcholinesterase (*h*AChE) inhibitor, into BACE-1 inhibition was achieved through introduction of backbone amide linkers to the designed compounds which are capable of hydrogen-bonding with BACE-1 catalytic site. *In vitro* assays and molecular modeling studies revealed the dual mode of action of compounds **4-6** against *h*AChE and BACE-1. Notably, compound **4** displayed potent *h*AChE inhibition (IC_{50} value of 4.11 nM) and BACE-1 inhibition (IC_{50} value of 18.3 nM) in comparison to donepezil (IC_{50} values of 6.21 and 194 nM against *h*AChE and BACE-1, respectively). Moreover, **4** revealed potential metal chelating property, low toxicity on SH-SY5Y neuroblastoma cells and ability to cross the blood-brain barrier (BBB) in PAMPA-BBB assay which renders **4** a potential lead for further optimization of novel small ligands for the treatment of Alzheimer's disease.

Keywords: Alzheimer's disease, Acetylcholinesterase, β -Secretase 1, Donepezil analogues, Permeability

1. Introduction

Alzheimer's disease (AD), a progressive neurodegenerative disease, is the most common cause of dementia in elderly people [1]. It is estimated that approximately one-third of people over 85 years of age are affected by AD. The dysfunction in basal forebrain cholinergic system is considered a hallmark of AD that is directly associated with memory impairment and cognitive deficit [2]. Consequently, the inhibition of acetylcholinesterase (AChE), an enzyme that catalyzes acetylcholine hydrolysis emerged as a valuable approach in the treatment of AD by improving the cholinergic functions in AD patients [3]. AChE inhibitors are still the only FDA-approved drugs as palliative therapeutics in the early symptomatic stage of AD [4]. Blocking the production of amyloid- β ($A\beta$) plaques is an alternative therapeutic approach for AD through the inhibition of β -secretase 1 (BACE-1) [5]. Extracellular cleavage of the amyloid precursor

protein (APP) by BACE-1 is the limiting step in the deposition of A β plaques in the brain which contributes significantly in the pathogenesis of AD [5]. The current complexity of AD therapy as well as poor efficacy of lead BACE-1 and AChE inhibitors have directed research towards identification of multi-target-directed ligands (MTDLs) as potential therapeutics of AD [6].

Donepezil, a potent and selective *h*AChE inhibitor, is a FDA-approved drug for treatment of mild to severe dementia in AD [7-9]. The potency and safety of donepezil have directed tremendous research efforts with the aim of designing donepezil analogues for AD therapy [10-12]. The X-ray crystal structure of donepezil with *h*AChE (PDB code: 4EY7) identified two main sites for receptor-ligand interactions: the catalytic anionic site (CAS) featuring Trp86, Tyr130, Tyr133, Phe 338 residues and the peripheral anionic site (PAS) including Trp286, Tyr341, Asp74 residues [13-16]. Analysis of donepezil binding to *h*AChE revealed dual interaction of donepezil with both CAS and PAS [17-19]. The indanone moiety of donepezil stacks against Trp286 residue in PAS, while the benzyl ring features π - π interaction with Trp 86 residue in CAS (Figure 1). Moreover, the carbonyl group of the indanone moiety is involved in hydrogen bonding with Phe295 residue.

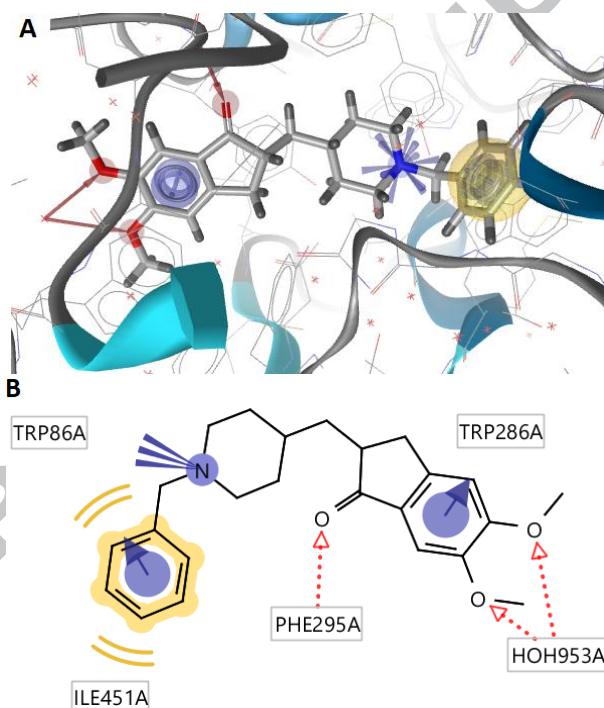


Figure 1. X-ray crystal structure of recombinant human acetylcholinesterase in complex with donepezil (PDB ID: 4EY7). (A) 3D binding pose. (B) 2D binding pose.

Structure-based design of *h*AChE inhibitors relying on donepezil as a lead shared the structural features displayed in Figure 2. The general structure of *h*AChE inhibitors revealed a methoxy-substituted aromatic ring that interacts with PAS of *h*AChE, a basic center that binds to CAS and a linker between these two fragments such as CH₂, CONH and CONHCH₂ [20-23].

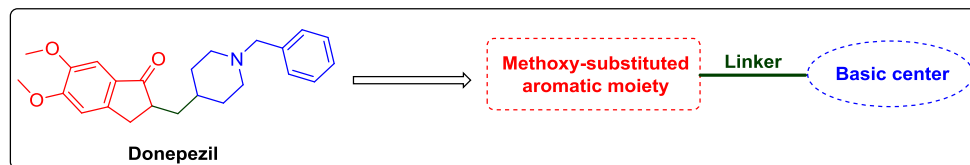


Figure 2. General structure of *hAChE* inhibitors based on donepezil.

Structure identification of BACE-1 with polypeptide inhibitors (PDB code: 1M4H) by X-ray diffraction supported structure-based approaches for BACE-1 inhibitors [24,25]. The Asp32 and Asp228 residues in BACE-1 play a key role in catalyzing the hydrolysis of amide bonds of APP, which are identified as catalytic sites of BACE-1 [26]. The isatin-based BACE-1 inhibitor (**I**, Figure 3), identified using a virtual high-throughput screening approach, displayed potent inhibition of BACE-1 with IC_{50} value of 2.4 μ M through hydrogen-bonding interactions with the catalytic aspartate residues [26]. This design strategy was further extended recently to identify BACE-1-based MTDLs through introduction of connecting amide bonds to isoquinoline derivatives to enable hydrogen bond formation with BACE-1 active site [27]. In the aim of development of potent MTDLs, the pharmacophoric features displayed by *hAChE* inhibitors were further tuned to incorporate other functional groups that can inhibit BACE-1. In this context, the multi-targeted coumarin derivative (**II**, Figure 3) exhibited dual AChE and BACE-1 submicromolar inhibitory potency [28]. Moreover, donepezil analogue (**III**, Figure 3) emerged as a potential lead for dual AChE/BACE-1 inhibitors owing to the structural rigidity caused by the double bond on the indanone moiety [29]. Development of MTDLs centered on BACE-1 is limited owing to the poor pharmacokinetic profile and CNS penetration ability of the lead compounds as well as the complexity of obtaining a balanced inhibitory profile against multiple targets [25, 30]. Based on these findings, research strategies have focused on development of hybrid molecules characterized by similarity to known AD drugs [31-33]. In this study, we report the synthesis and evaluation of donepezil analogues that maintain the general structural features required for *hAChE* inhibition (Figure 2). In addition, backbone amide linkers are introduced to the donepezil template to maximize BACE-1 inhibition through hydrogen-bonding interactions with the catalytic aspartate residues based on previous findings [26, 27]. Moreover, amide linkers are proposed to introduce metal chelating ability to the designed ligands which represents a vital therapeutic approach for AD. The effectiveness of the design strategy was further validated *via* evaluation of analogues lacking the backbone amide bonds. Molecular modeling studies were employed to investigate the dual interaction mechanism of the new compounds with *hAChE* and BACE-1. In addition, the ability of the new compounds identified in this study to cross the blood-brain barrier (BBB) and their effect on viability of SH-SY5Y neuroblastoma cells were further evaluated.

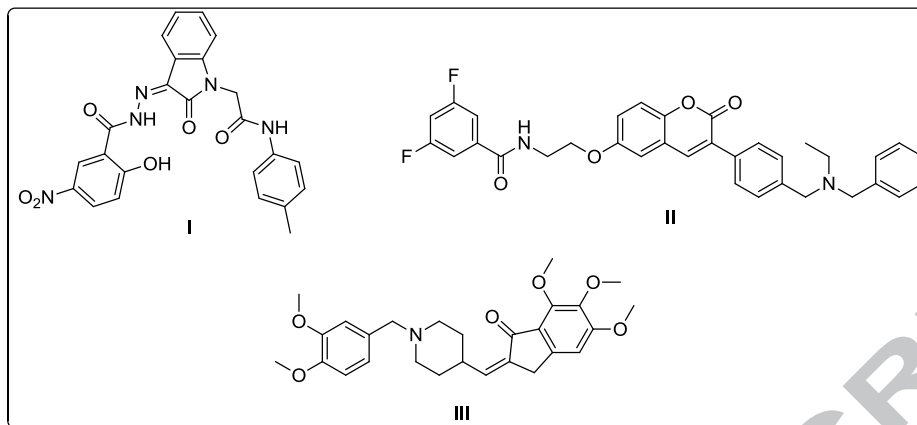
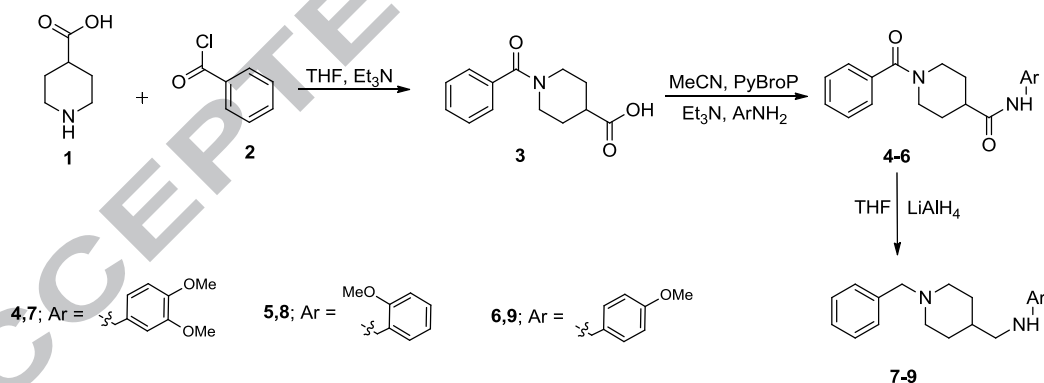


Figure 3. Chemical structures of compounds I-III.

2. Results and Discussion

2.1. Chemistry

A general approach for the synthesis of the designed compounds is outlined in Scheme 1. As shown in Scheme 1, the starting isonipecotic acid **1** reacted with benzoyl chloride **2** under microwave irradiation to afford compound **3** in a good yield. Further coupling of **3** with substituted benzylamines under microwave irradiation proceeded smoothly to furnish target compounds **4-6** in serviceable yields. Moreover, refluxing **4-6** and lithium aluminum hydride in tetrahydrofuran yielded compounds **7-9** (Scheme 1).



Scheme 1.

2.2. Dual *h*AChE and BACE-1 inhibitory activities

The biological effect of the synthesized compounds **4-9** has been assessed for their inhibitory activities exerted on the *in vitro* *h*AChE and BACE-1 activities. To test the preliminary inhibition power, the *h*AChE and BACE-1 activities were measured in the absence or in the presence of 0.1 μ M of compounds **4-9** and donepezil (Figure 4 and 5). The results reported in

Figure 4 revealed that compound **4** exhibited the greatest inhibitory activity on *hAChE* which was greater than that exhibited by donepezil. In addition, compounds **5** and **6** demonstrated comparable potency to donepezil in terms of inhibitory activity on *hAChE*. Such finding clearly demonstrate the importance of the 3,4-dimethoxy substitution pattern of **7** on the *hAChE* inhibitory effect of the tested compounds. Moreover, compounds **7-9** revealed generally lower activity as *hAChE* inhibitors which reveals that the amide bonds play a key role in the interaction with the target receptor. In Table 1, the inhibitory potency of **4-9** on *hAChE* is expressed as IC_{50} , which represents the concentration of inhibitor required to decrease the enzyme activity by 50%. Compound **4**, the most active member of this study displayed IC_{50} value of 4.11 nM in comparison to IC_{50} value of 6.21 nM for donepezil.

The effect of **4-9** on BACE-1 activity was compared to that exhibited by donepezil (Figure 5). Interestingly, compounds **4-6** exhibited potent BACE-1 inhibitory activity at 0.1 μ M in contrast to the effect of donepezil. It is noteworthy to mention that the comparable potency of **4-6** as BACE-1 inhibitors suggests that the substitution pattern of the methoxy groups on the benzyl moiety has no influence on potential interaction with BACE-1. However, compounds **7-9** lacking the backbone amide linkers displayed negligible BACE-1 inhibitory activity at 0.1 μ M in agreement with our proposed hypothesis. The IC_{50} values of **4-6** as BACE-1 were in the range of 18.3-19.1 nM which further confirmed their potency in comparison to IC_{50} value of 194 nM for donepezil. These results further validate our hypothesis of tailoring donepezil template to BACE-1 inhibitory activity through the introduction of backbone amide linkers in **4-6**. Compound **4** displayed better dual activity and lower IC_{50} values against both *hAChE* and BACE-1 than the FDA-approved donepezil.

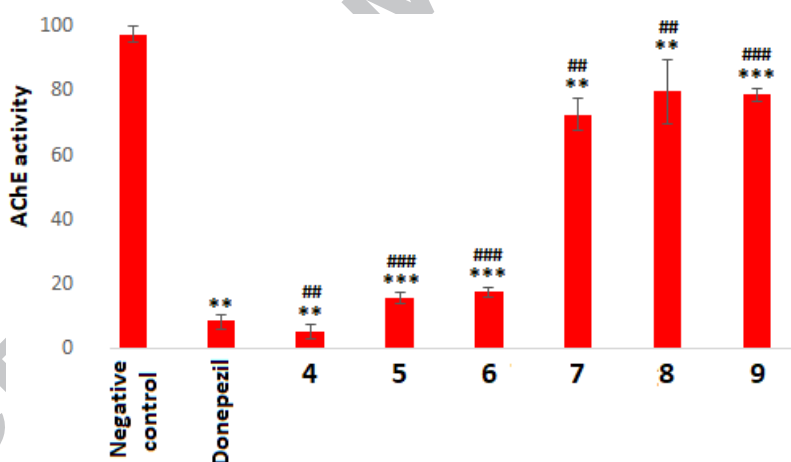


Figure 4. AChE activity determined in the presence of donepezil and compounds **4-9** (0.1 μ M). Negative control represents AChE activity in the absence of the tested compounds. The data represents the average of three different determinations with indication of the standard error, (** $p < 0.05$, vs control; *** $p < 0.01$ vs. control; ## $p < 0.05$, vs donepezil; ### $p < 0.01$ vs. donepezil (ANOVA)).

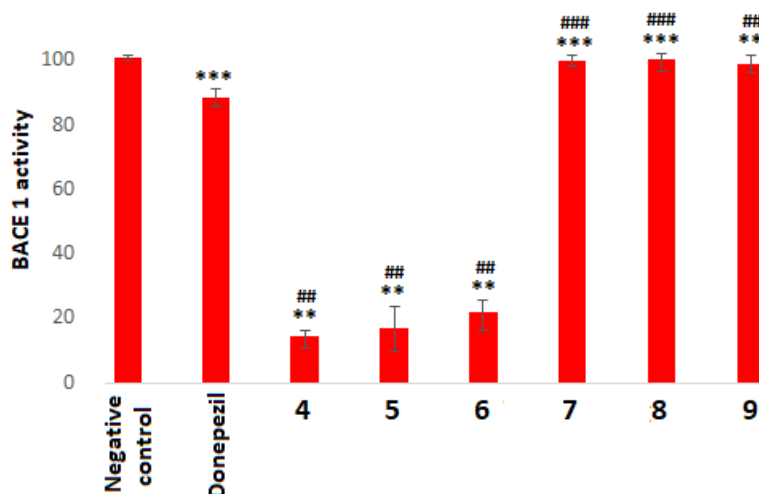


Figure 5. BACE-1 activity determined in the presence of donepezil and compounds **4-9** (0.1 μ M). Negative control represents BACE-1 activity in the absence of the tested compounds. The data represents the average of three different determinations with indication of the standard error. (** $p < 0.05$, vs control; *** $p < 0.01$ vs. control; ## $p < 0.05$, vs donepezil; ### $p < 0.01$ vs. donepezil (ANOVA)).

Table 1. IC₅₀ values (nM) of compounds **4-9** for their AChE and BACE-1 inhibitory activity.

Comp.	AChE IC ₅₀ (nM) ^a	BACE-1 IC ₅₀ (nM) ^a
4	4.11 ± 0.12	18.3 ± 0.17
5	8.46 ± 0.23	18.5 ± 0.13
6	9.78 ± 0.14	19.1 ± 0.06
7	145 ± 1.42	243 ± 1.13
8	157 ± 2.43	277 ± 2.11
9	165 ± 1.75	253 ± 1.62
Donepezil	6.21 ± 0.04	194 ± 1.24
BACE-1 inhibitor IV	Nd ^b	15.1 ± 0.06

Bold values represent best results.

^aData are shown as mean values \pm standard deviation (n=3); ^bNd; not determined.

2.3. *In vitro* cytotoxicity testing

The effect of compounds **4-6** on cell viability was assessed in SH-SY5Y neuroblastoma cells. Compounds **4-6** did not affect SH-SY5Y cells viability, in comparison with the untreated controls and rotenone as a positive control (Figure 6). Further screening at 10-dose level revealed that **4-6** possessed IC₅₀ values of $>50 \mu$ M against SH-SY5Y neuroblastoma cells. These results demonstrate the potential utility of these compounds as leads for development of therapeutics for neurological diseases.

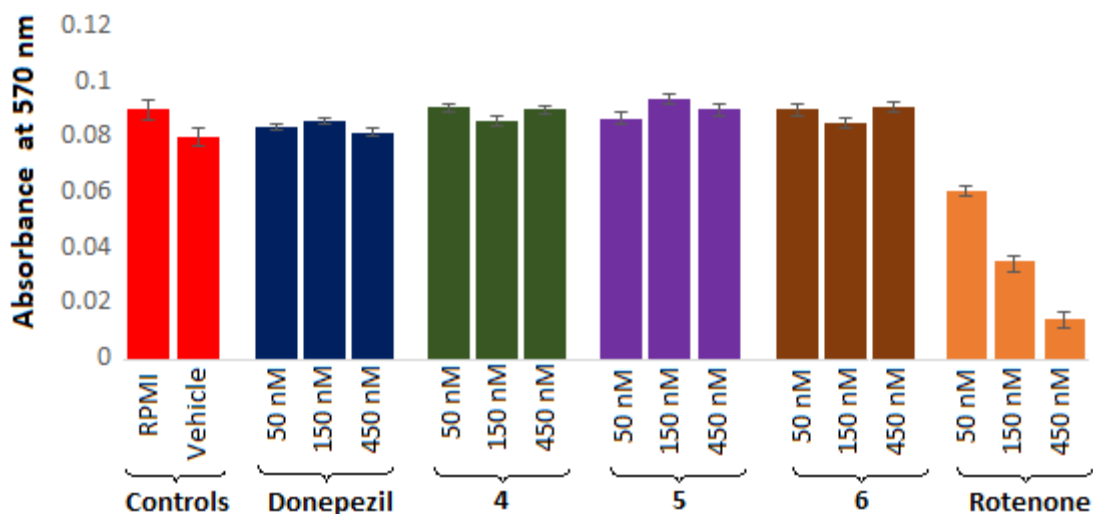
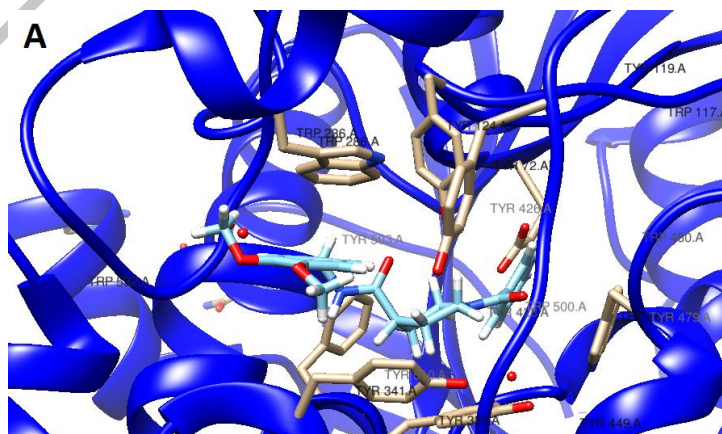


Figure 6. The effect of donepezil, compounds **4-6** and rotenone on SH-SY5Y cells viability at three different concentrations. As controls, RPMI medium in the absence or in the presence of 0.1% DMSO, were used.

2.4. Molecular modeling

In order to get an insight into the dual interaction mechanism of **4** with *hAChE* and BACE-1, a molecular docking study based on the X-ray crystal structures of *hAChE* (PDB code 4EY7) and BACE-1 (PDB code 1M4H) was carried out. The results of the docking study using *hAChE* (PDB code 4EY7) as shown in Figures 7A & 7B indicated that compound **4** covered the binding gorge in a satisfactory orientation comparable to that of donepezil resulting in potent *hAChE* inhibitory activity. The dimethoxy substituted benzyl moiety occupied the PAS of *hAChE* interacting by π - π stacking with Trp286 and Tyr341 residues. Similarly to donepezil, Phe295 residue of *hAChE* was involved in hydrogen bonding with the amide bond of **4**. In addition, the piperidinyll moiety established hydrophobic interactions with Phe297, Phe338 and Tyr124 residues in the CAS of *hAChE* (Figure 7).



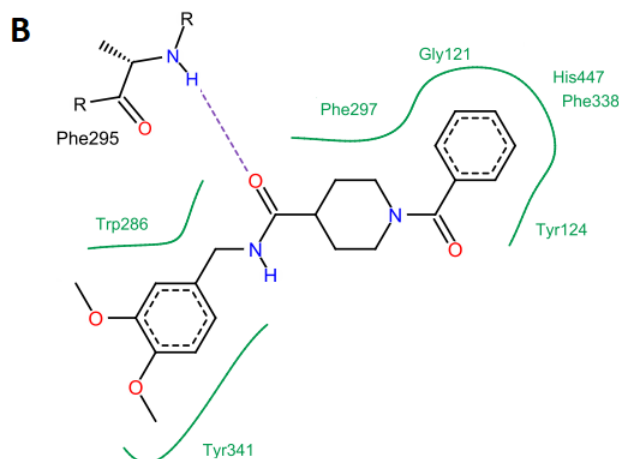


Figure 7. (A) 3D Interaction of compound **4** with the binding site of *hAChE* (PDB code 4EY7). The atoms are colored as following: red for oxygen atoms, blue for nitrogen atoms, white for hydrogen atoms and cyan for carbon atoms. (B) 2D Interaction of compound **4** with the binding site of *hAChE* (PDB code 4EY7). Dashed lines represent hydrogen bonds. Hydrophobic interactions are shown by green solid lines.

Moreover, compound **4** displayed preferential binding to BACE-1 (PDB code 1M4H) with estimated binding energy of $-18.76 \text{ kcal mol}^{-1}$ which comes in good agreement with *in vitro* BACE-1 inhibitory assay. The detailed analysis of the binding interaction is displayed in the 2D binding mode of **4** in Figure 8. The piperidinyll moiety of **4** is stretched into a pocket of the target enzyme revealing interactions with Gly11, Ile110 and Gln12 residues. The dimethoxy substituted benzyl moiety of **4** was involved in π - π stacking with Tyr71 and Tyr198 residues. In addition, the amide linkers in **4** displayed hydrogen bonding with Asp228, Thr232 and Thr72 residues of the catalytic site of BACE-1. In addition, the binding mode of donepezil to BACE-1 (PDB code 1M4H) was examined. The 2D binding interaction of donepezil displayed in Figure 9 revealed interaction of donepezil with hydrogen bonding to Thr232 and Thr72 residues. Lacking hydrogen bonding interaction with Asp228 residue for donepezil further validates its key role in maximizing the *in vitro* potency of compound **4** against BACE-1 in comparison to donepezil. Similarly to compound **4**, donepezil displayed π - π stacking with Tyr71 and Tyr198 residues. Taking into consideration the analysis of the docking results and *in vitro* enzymatic assays, it was confirmed that compound **4** was a dual inhibitor of *hAChE* and BACE-1.

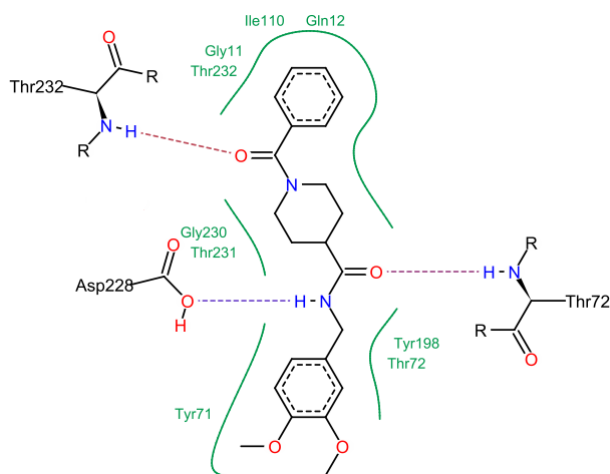


Figure 8. 2D Interaction of compound **4** with the active site of BACE-1 (PDB code 1M4H). Dashed lines represent hydrogen bonds. Hydrophobic interactions are shown by green solid lines.

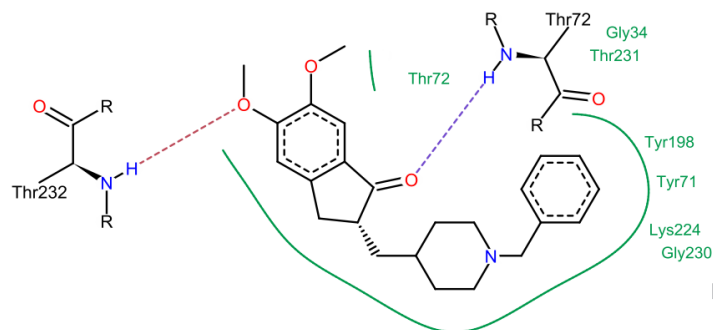


Figure 9. 2D Interaction of donepezil with the active site of BACE-1 (PDB code 1M4H). Dashed lines represent hydrogen bonds. Hydrophobic interactions are shown by green solid lines.

2.5. *In vitro* blood-brain barrier permeability

In the process of development of therapeutics for neurological diseases, the ability of a drug to permeate the blood–brain barrier (BBB) is a crucial property for central nervous system (CNS) drugs. The parallel artificial membrane permeability assay for BBB (PAMPA-BBB) is a high throughput technique used to evaluate the ability of small molecules to transverse the BBB expressed as effective permeability (P_e , cm/s) [34]. Assay validation was performed by comparing the P_e values of compounds **4-6** to that of caffeine as a low passive permeability drug and donepezil as a high passive permeability drug. Based on the P_e values obtained (Table 2), compounds **4-6** showed high passive permeability with P_e values ranging from 20.13 to 22.97 $\times 10^{-6}$ cm/s which is comparable to P_e value of donepezil 23.35 $\times 10^{-6}$ cm/s. Moreover, the lipophilicity of a drug is considered a critical parameter that affects its pharmacokinetic properties. Compounds with moderate lipophilicity (Log $D_{7.4}$ 0–3) possess a good balance between solubility and permeability required for oral absorption and cell membrane permeation in cell-based assays [35]. In general, CNS drugs possess (Log $D_{7.4}$ ~2) which is optimal for BBB penetration and low metabolic liability. To examine the likelihood of success of the investigated compounds **4-6**, their Log $D_{7.4}$ were experimentally determined using shake flask method (Table 2). Compounds **4-6** displayed optimal (Log $D_{7.4}$ ~2) required for CNS drugs which renders them potential leads for further development as AD therapeutics.

Table 2. PAMPA-BBB permeability ($P_e \times 10^{-6}$ cm s⁻¹) of **4-6** and controls expressed as P_e , their lipophilicities at pH 7.4 (Log $D_{7.4}$) and their predictive penetration to the CNS.

Comp.	P_e ($\times 10^{-6}$ cm s ⁻¹)	Log $D_{7.4}$	Prediction of CNS penetration
4	20.13	2.27	High
5	22.43	2.43	High
6	22.97	2.49	High
Donepezil	23.35	2.71	High
Caffeine	2.24	-0.63	Low

2.6. Metal chelating ability

Numerous studies reported higher levels of biometals such as Cu^{2+} and Zn^{2+} in an AD brain compared to healthy brain [36-38]. These results suggested that destruction of the balance of metal ions in CNS is an underlying cause of neurodegenerative diseases. Indeed, several lead compounds with metal-chelating property have displayed promising potential as AD therapeutics [39-41]. These findings directed us to postulate that incorporation of amide linkers in the designed compounds could introduce metal-chelating property that would be useful in the design of MTDLs for AD treatment. The metal chelating property of compound **4** was examined by recording its UV-visible absorption spectra with wavelength ranging from 200 to 500 nm in the presence of increasing concentrations of Cu^{2+} . The differential absorption spectra obtained upon incremental addition of Cu^{2+} (5-50 μM) to **4** revealed remarkable hyperchromic effect which accounts for potential interaction between **4** and Cu^{2+} (Figure 10). These results indicate that **4** could effectively chelate Cu^{2+} , and thereby could serve as a metal chelator in treating AD. The metal chelating property of **4** is attributed to the presence of the amide bonds as well as the dimethoxy groups.

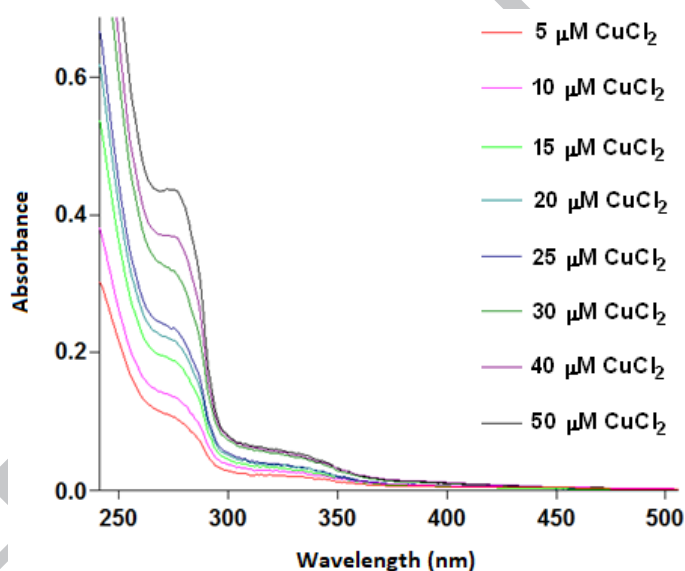


Figure 10. Differential UV-vis absorption spectra of compound **4** (25 μM) in methanol in the presence of increasing concentrations of CuCl_2 (5-50 μM). The differential spectra were obtained by subtraction of the mixture absorption spectra from the spectra of the free ligand and CuCl_2 at the corresponding concentration.

3. Conclusion

There is a pressing need to develop MTDLs for neurodegenerative diseases that combine structural requirements for potency with the strict need of tolerable toxicity and BBB permeation. In a summary, donepezil analogues are introduced in this study as dual *hAChE* and BACE-1 inhibitors which are considered promising MTDLs as therapeutics for neurodegenerative diseases. Profiling the donepezil template with potent *hAChE* inhibitor to exert BACE-1 inhibition was achieved through introduction of backbone amide bonds to compounds **4-6** which

are capable of hydrogen-bonding to the active site of BACE-1. In preliminary biological screening, compounds **4-6** maintained excellent *hAChE* inhibitory activity comparable to the FDA-approved drug, donepezil. In addition, **4-6** exhibited significantly superior BACE-1 inhibition compared to donepezil. The corresponding analogues **7-9** lacking the amide linkers displayed minimal inhibitory activity against BACE-1 which demonstrated the key role of the amide bonds in the interaction with the target receptor. The optimal candidate compound **4**, exhibited IC₅₀ values of 4.11 and 18.3 nM against *hAChE* and BACE-1, respectively. Moreover, **4** displayed potential biometal-chelating ability, high permeability in PAMPA-BBB assay and no effect on the viability of SH-SY5Y neuroblastoma cells in its effective concentration. Molecular modeling studies further revealed the dual binding capability of **4** to the active sites of *hAChE* and BACE-1. The lead compounds identified in this investigation proved to be promising scaffolds for the development of new potent multitarget compounds for neurological diseases.

4. Experimental

4.1. Chemistry

All commercially available starting materials, reagents, and solvents were used as supplied, unless otherwise stated. Reported yields are isolated yields. Purification of all final products was accomplished by silica gel flash column chromatography. Chloroform : methanol or hexane : ethyl acetate were used as elution solvents. Proton (¹H) and carbon (¹³C) NMR were collected on Bruker NMR spectrometer at 400 MHz for ¹H and 100 MHz for ¹³C. Chemical shifts (δ) are reported in parts-per million (ppm) relative to residual undeuterated solvent. Melting points were recorded using a capillary melting point apparatus and are uncorrected. High resolution mass spectra were obtained using electron spray ionization (ESI). Purity (>95%) of compounds **4-9** was confirmed by analytical HPLC.

4.1.1. 1-Benzoylpiperidine-4-carboxylic acid (**3**)

A mixture of isonipecotic acid **1** (129 mg, 1.0 mmol), benzoyl chloride **2** (140 mg, 1.0 mmol) and Et₃N (0.32 mL, 2.5 mmol) in THF (5 mL) was stirred under microwave irradiation (120 W) at 70 °C for 15 min. The reaction mixture was acidified using 1M HCl (10 mL) and extracted with dichloromethane (3× 25 mL). The combined organic layers were dried over anhydrous Na₂SO₄, filtered, and concentrated under reduced pressure. The crude product was purified by flash column chromatography using 5% ethyl acetate in hexane, followed by 80% ethyl acetate in hexane as eluent to yield **3** (94%) as white solid. Mp 136-138°C. ¹H NMR (400 MHz, CDCl₃) δ 1.71-1.85 (m, 3H), 2.03-2.06 (m, 1H), 2.59 (tt, 1H, *J* = 10.4, 4.1 Hz), 3.04-3.12 (m, 2H), 3.72-3.76 (m, 1H), 4.48-4.52 (m, 1H), 7.36-7.44 (m, 5H), 11.16 (br s, 1H). ¹³C NMR (100 MHz, CDCl₃) δ 40.4, 41.4, 46.8, 126.7, 128.3, 129.6, 135.3, 170.7, 178.3. HRMS (ESI): calcd for C₁₃H₁₄NO₃ [M-H]⁻, 232.0973; found, 232.0979.

4.1.2. 1-Benzoyl-*N*-(3,4-dimethoxybenzyl)piperidine-4-carboxamide (**4**)

To a solution of compound **3** (233 mg, 1.0 mmol) in MeCN (4 mL), PyBroP (466 mg, 1.0 mmol) and Et₃N (0.32 mL, 2.5 mmol) were added and stirred at room temperature for 10 mins. A solution of 3,4-dimethoxybenzylamine (167 mg, 1.0 mmol) in MeCN (3 mL) was then added and the reaction mixture stirred under microwave irradiation (80 W) at 90 °C for 20 min. The

solvent was removed under reduced pressure, and the crude mixture was suspended in H₂O (20 mL) and extracted with dichloromethane (2× 20 mL). The combined organic layers were dried over anhydrous Na₂SO₄, filtered, and concentrated under reduced pressure. The crude product was purified by flash column chromatography using 10% ethyl acetate in hexane, followed by 50% ethyl acetate in hexane as eluent to yield **4** (91%) as yellowish white solid. Mp 177-179°C. ¹H NMR (400 MHz, CDCl₃) δ 1.63-1.81 (m, 3H), 2.27-2.33 (m, 2H), 2.71-2.86 (m, 2H), 3.67-3.71 (m, 1H), 3.77 (s, 3H), 3.78 (s, 3H), 4.25 (d, 2H, *J* = 5.4 Hz), 4.52-4.56 (m, 1H), 6.68-6.75 (m, 3H), 7.10-7.19 (m, 2H), 7.25-7.35 (m, 3H). ¹³C NMR (100 MHz, CDCl₃) δ 41.3, 42.5, 42.8, 46.8, 55.5, 55.6, 110.9, 119.6, 126.4, 127.9, 128.2, 128.7, 129.4, 135.6, 148.0, 148.7, 170.0, 173.7. HRMS (ESI): calcd for C₂₂H₂₇N₂O₄ [M+H]⁺, 383.1970; found, 383.1967.

4.1.3. 1-Benzoyl-*N*-(2-methoxybenzyl)piperidine-4-carboxamide (**5**)

Using the procedure given for the preparation of **4**, coupling of **3** (233 mg, 1.0 mmol) and 2-methoxybenzylamine (137 mg, 1.0 mmol) gave **5** (87%) as pale yellow solid after purification by flash column chromatography using 40% ethyl acetate in hexane as eluent. Mp 152-153°C. ¹H NMR (400 MHz, CDCl₃) δ 1.52-1.75 (m, 4H), 2.26-2.32 (m, 1H), 2.31-2.81 (m, 2H), 3.61-3.66 (m, 1H), 3.70 (s, 3H), 4.28 (d, 2H, *J* = 5.6 Hz), 4.46-4.51 (m, 1H), 6.74-6.81 (m, 2H), 6.90 (t, 1H, *J* = 5.7 Hz), 7.08-7.16 (m, 2H), 7.22-7.32 (m, 5H). ¹³C NMR (100 MHz, CDCl₃) δ 38.1, 38.2, 42.2, 46.7, 54.8, 109.8, 120.0, 125.9, 126.2, 128.0, 128.1, 128.3, 129.1, 135.6, 156.8, 169.8, 173.6. HRMS (ESI): calcd for C₂₁H₂₅N₂O₃ [M+H]⁺, 353.1865; found, 353.1871.

4.1.4. 1-Benzoyl-*N*-(4-methoxybenzyl)piperidine-4-carboxamide (**6**)

Using the procedure given for the preparation of **4**, coupling of **3** (233 mg, 1.0 mmol) and 4-methoxybenzylamine (137 mg, 1.0 mmol) gave **6** (82%) as yellowish white solid after purification by flash column chromatography using 50% ethyl acetate in hexane as eluent. Mp 188-191°C. ¹H NMR (400 MHz, CDCl₃) δ 1.62-1.82 (m, 4H), 2.27-2.32 (m, 1H), 2.82-2.87 (m, 2H), 3.65-3.69 (m, 1H), 3.73 (s, 3H), 4.26 (d, 2H, *J* = 5.7 Hz), 4.52-4.57 (m, 1H), 6.50 (br s, 1H), 6.79 (d, 2H, *J* = 8.4 Hz), 7.10 (d, 2H, *J* = 8.4 Hz), 7.24-7.36 (m, 5H). ¹³C NMR (100 MHz, CDCl₃) δ 41.3, 42.5, 42.7, 47.0, 55.1, 113.8, 126.5, 128.3, 128.8, 129.5, 130.3, 135.8, 158.7, 170.2, 173.7. HRMS (ESI): calcd for C₂₁H₂₅N₂O₃ [M+H]⁺, 353.1865; found, 353.1869.

4.1.5. 1-(1-Benzylpiperidin-4-yl)-*N*-(3,4-dimethoxybenzyl)methanamine (**7**)

To a solution of **4** (382 mg, 1.0 mmol) in THF (8 mL), LiAlH₄ (189 mg, 5.0 mmol) was added at 0°C. The reaction mixture was refluxed for 6 hrs, then it was cooled to room temperature and quenched with H₂O (10 mL) and extracted with dichloromethane (2× 10 mL). The combined organic layers were dried over anhydrous Na₂SO₄, filtered, and concentrated under reduced pressure. The crude product was purified by flash column chromatography using 30% ethyl acetate in hexane to yield **7** (76%) as yellow solid. Mp 144-146°C. ¹H NMR (400 MHz, CDCl₃) δ 1.21-1.28 (m, 3H), 1.65-1.70 (m, 2H), 1.89-1.94 (m, 2H), 2.48 (d, 2H, *J* = 6.7 Hz), 2.83-2.87 (m, 2H), 3.45 (s, 2H), 3.69 (s, 2H), 3.83 (s, 3H), 3.85 (s, 3H), 6.77-6.80 (m, 2H), 6.86 (s, 1H), 7.23-7.31 (m, 5H). ¹³C NMR (100 MHz, CDCl₃) δ 30.5, 36.0, 53.5, 53.7, 55.2,

55.7, 55.8, 63.3, 110.8, 111.1, 119.9, 126.7, 128.0, 129.0, 133.0, 138.4, 147.8, 148.8. HRMS (ESI): calcd for C₂₂H₃₁N₂O₂ [M+H]⁺, 355.2385; found, 355.2388.

4.1.6. 1-(1-Benzylpiperidin-4-yl)-N-(2-methoxybenzyl)methanamine (8)

Using the procedure given for the preparation of **7**, compound **5** (352 mg, 1.0 mmol) and LiAlH₄ (189 mg, 5.0 mmol) gave **8** (69%) as yellowish white solid after purification by flash column chromatography using 40% ethyl acetate in hexane as eluent. Mp 135-136°C. ¹H NMR (400 MHz, CDCl₃) δ 1.26-1.34 (m, 2H), 1.48-1.53 (m, 1H), 1.70-1.75 (m, 2H), 1.94-1.99 (m, 2H), 2.49-2.54 (m, 2H), 2.90 (d, 2H, *J* = 6.5 Hz), 3.50 (s, 2H), 3.80 (s, 2H), 3.83 (s, 3H), 6.84-6.98 (m, 2H), 7.23-7.35 (m, 7H). ¹³C NMR (100 MHz, CDCl₃) δ 30.4, 36.0, 49.3, 53.3, 53.6, 55.0, 63.3, 110.0, 120.2, 122.4, 126.7, 127.9, 128.0, 129.0, 129.5, 138.5, 157.4. HRMS (ESI): calcd for C₂₁H₂₉N₂O [M+H]⁺, 325.2279; found, 325.2284.

4.1.7. 1-(1-Benzylpiperidin-4-yl)-N-(4-methoxybenzyl)methanamine (9)

Using the procedure given for the preparation of **7**, compound **6** (352 mg, 1.0 mmol) and LiAlH₄ (189 mg, 5.0 mmol) gave **9** (71%) as yellowish white solid after purification by flash column chromatography using 50% ethyl acetate in hexane as eluent. Mp 150-151°C. ¹H NMR (400 MHz, CDCl₃) δ 1.25-1.35 (m, 2H), 1.49-1.53 (m, 1H), 1.70-1.74 (m, 2H), 1.94-2.01 (m, 2H), 2.53 (d, 2H, *J* = 6.7 Hz), 2.90-2.93 (m, 2H), 3.51 (s, 2H), 3.74 (s, 2H), 3.82 (s, 3H), 6.89 (d, 2H, *J* = 8.5 Hz), 7.26 (d, 2H, *J* = 8.5 Hz), 7.31-7.37 (m, 5H). ¹³C NMR (100 MHz, CDCl₃) δ 30.5, 36.1, 53.4, 53.6, 55.1, 55.2, 63.4, 113.6, 126.7, 128.0, 129.0, 129.1, 132.6, 138.5, 158.4. HRMS (ESI): calcd for C₂₁H₂₉N₂O [M+H]⁺, 325.2279; found, 325.2282.

4.2. Biological Testing

4.2.1. Dual hAChE and BACE-1 inhibitory activities

Inhibitory activity of the synthesized compounds against AChE was measured using the spectrophotometric Ellman's method [42]. Human recombinant AChE was obtained from Sigma Aldrich. Acetylthiocholine (ATC) and 5,5'-dithio-bis(2-nitrobenzoic acid) (DTNB) were purchased from Sigma Aldrich and stock solutions of 0.01 M in H₂O were prepared. Enzymatic hydrolysis of ATC was monitored by UV-visible absorption at 412 nm in the presence and absence of various concentrations of inhibitors at 25 °C in 0.1 M potassium phosphate, pH 7.0. To determine the IC₅₀ value, six different concentrations of each compound were used to obtain enzyme activities between 5% and 95%. All reactions were performed in triplicate. The IC₅₀ values were calculated using nonlinear regression (GraphPad Prism 5 (GraphPad Software, San Diego, CA, USA, 5.00)) by plotting the residual enzyme activities against the applied inhibitor concentration.

All the compounds were tested as BACE-1 inhibitors using a PanVera's BACE-1 fluorescence resonance energy transfer (FRET) assay kit [43, 44]. The analyses were carried out according to the supplied protocol. The wavelength was optimized for 553 nm excitation and 576 nm for emission monitoring. Stock solutions of the tested compounds were prepared in DMSO and further diluted with assay buffer (50 mM sodium acetate; pH 4.5). 10 μL of BACE-1 substrate

(750 nM) was mixed with 10 μ L of test compound (or assay buffer; i.e., blank sample), then 10 μ L of BACE-1 (1 Unit/mL) was added to start the reaction. After 60 min of incubation at 25 $^{\circ}$ C, 10 μ L of 2.5 M sodium acetate was added to stop the reaction. The emission signal was monitored at 576 nm. Inhibition percentage was calculated from $[1 - (S_{60} - S_0)/(C_{60} - C_0)] \times 100$, where S_0 and S_{60} are the fluorescence intensities of the test sample (enzyme, substrate, test compound) at the beginning of the reaction and after 60 min, respectively, while C_0 and C_{60} are the analogical fluorescence intensities of the blank sample (enzyme, substrate, buffer). Each compound was analyzed in triplicate. BACE-1 Inhibitor IV (Cayman Chemical) was used as a reference compound. ANOVA (analysis of variance) assay was conducted to evaluate the difference between the experiment and control groups. Significance was set at $p < 0.05$.

4.2.2. Cell viability assay

SH-SY5Y neuroblastoma cells were grown in Roswell Park Memorial Institute medium (RPMI) supplemented with 2 mM L-glutamine, 100 UI/mL penicillin, 100 μ g/mL streptomycin and 10% (v/v) fetal bovine serum (FBS). Cells were maintained in culture dishes at 37 $^{\circ}$ C in a saturated humidity atmosphere containing 95% air and 5% CO₂. Cells were seeded at an initial density of 104 cells/cm² in culture dishes. At a confluence of 80%, cells were detached by trypsin (0.25%) treatment for 2 min, suspended in fresh medium without FBS and transferred to 96-multiwell (1 \times 10⁴ cells/well). After 24 h from seeding, cells were incubated in the absence or in the presence of the 3 different concentrations (50, 150 and 450 nM) of compounds **4-6**, donepezil and rotenone. The viability of the cells was evaluated after 48 h treatment as mitochondrial activity using the MTT assay [45-47]. Briefly, after the treatment the medium was removed and cells were incubated with 100 μ l MTT (3-(4,5-dimethylthiazole-2-yl)-2,5-diphenyltetrazolium bromide) (0.5 mg/ml) for 1 h. After that, the solution was removed, the formazan formed solubilized in 100 μ l of 0.1N HCl in 90 % (v/v) 2-propanol and the absorbance measured at 570 nm using a microplate reader (BioRad 680, USA). Results were expressed as absorbance values at 570 nm of the treated cells vs. control cells.

4.3. Molecular modeling studies

The 2D structures of compound **4** and donepezil were built and converted into the 3D using vLife MDS 3.0 software. The 3D structures were then energetically minimized up to the rms gradient of 0.01 using the CHARMM22 force field. All conformers were then energetically minimized up to the rms gradient of 0.01. Molegro software was used for molecular docking studies and Lead IT software was used to generate 2D binding poses of compound **4** and donepezil.

4.4. *In vitro* blood-brain barrier permeability

The ability of the investigated compounds to penetrate into blood-brain barrier was evaluated using a parallel artificial membrane permeation assay (PAMPA) for blood-brain barrier according to the method established by Di *et al.* [35]. Donepezil and caffeine were used as reference compounds in the PAMA assay. The donor microplate (96-well filter plate, PVDF membrane) and the acceptor microplate (indented 96-well plate) were both obtained from Millipore. The acceptor 96-well microplate was filled with 300 μ L of PBS/EtOH (7:3), and the filter membrane was

impregnated with 10mL of PBL in dodecane (20 mg/mL). The compound was dissolved in DMSO at a concentration of 5 mg/mL followed diluting 50-fold with a mixture of PBS/EtOH (7:3) to give a final concentration of 100 µg/mL. After that, 200 µL of diluted solution and 300 µL of PBS/EtOH (7:3) were added to the donor wells. The donor filter plate was placed on the acceptor plate to make the underside of filter membrane in contact with buffer solution. After leaving this sandwich assembly for 16 h at 25 °C, the donor plate was removed, and the concentrations of tested compound in the acceptor, donor and reference wells were measured with a UV plate reader. Each sample was analyzed three independent runs in four wells. Log $D_{7.4}$ values were obtained using shake flask method as previously reported [35].

4.5. Metal chelation property

The study of metal chelation was performed in methanol at 25 °C using SHIMADZU UV-vis spectrophotometer with wavelength ranging from 200 to 500 nm. The absorption spectra of compound **4** (25 µM, final concentration) alone or in the presence of CuCl₂ (5-50 µM) for 30 min in methanol were recorded in quartz cells.

References

- [1] A.F. Jorm, D. Jolley, *Neurology*, 51 (1998) 728-733. DOI: <https://doi.org/10.1212/WNL.51.3.728>
- [2] P. T. Francis, A. M. Palmer, M. Snape, G. K. Wilcock, *J. Neurol. Neurosurg. Psychiatry* 66 (1999) 137-147. DOI: <http://dx.doi.org/10.1136/jnnp.66.2.137>
- [3] A. P. Murray, M. B. Faraoni, M. J. Castro, N. P. Alza, V. Cavallaro, *Curr. Neuropharmacol.* 11 (2013) 388-413. DOI:10.2174/1570159X11311040004
- [4] A. Leinonen, M. Koponen, S. Hartikainen, *PloS one* 10 (2015) e0124500. DOI:10.1371/journal.pone.0124500
- [5] C. Ridler, *Nat. Rev. Neurol.* 14 (2018) 126. DOI:10.1038/nrneurol.2018.12
- [6] S. Rizzo, C. Riviere, L. Piazzzi, A. Bisi, S. Gobbi, M. Bartolini, V. Andrisano, F. Morroni, A. Tarozzi, J.P. Monti, A. Rampa, *J. Med. Chem.* 51 (2008) 2883-2886. DOI:10.1021/jm8002747
- [7] H. Sugimoto, Y. Yamanishi, Y. Iimura, Y. Kawakami, *Curr. Med. Chem.* 7 (2000) 303-339. DOI: 10.2174/0929867003375191
- [8] E. A. Van der Zee, B. Platt, G. Riedel, *Behav. Brain Res.* 221 (2011) 583-586. DOI: 10.1016/j.bbr.2011.01.050
- [9] S. L. Rogers, R. S. Doody, R. C. Mohs, L. T. Friedhoff, *Arch. Intern. Med.* 158 (1998) 1021-1031. DOI:10.1001/archinte.158.9.1021
- [10] K. O. Yerdelen, M. Koca, B. Anil, H. Sevindik, Z. Kasap, Z. Halici, K. Turkyaydin, G. Gunesacar, *Bioorg. Med. Chem.* 25 (2015) 5576-5582. DOI: 10.1016/j.bmcl.2015.10.051
- [11] J. L. Marco, C. Rios, A. G. Garcia, M. Villarroya, M. C. Carreiras, C. Martins, A. Eleuterio, A. Morreale, M. Orozco, F. J. Luque, *Bioorg. Med. Chem.* 12 (2004) 2199-2218. DOI:10.1016/j.bmc.2004.02.017
- [12] R. Azzouz, L. Peauger, V. Gembus, M.-L. Tintas, J. S. O. Santos, C. Papamicael, V. Levacher, *Eur. J. Med. Chem.* 145 (2018) 165-190. DOI: 10.1016/j.ejmech.2017.12.084
- [13] S.S. Xie, J.S. Lan, X.B. Wang, N. Jiang, G. Dong, Z.R. Li, K.D.G. Wang, P.P. Guo, L.Y. Kong, *Eur. J. Med. Chem.* 93 (2015) 42-50. DOI: 10.1016/j.ejmech.2015.01.058

- [14] M.B. Colovic, D. Krstic, T. Lazarevic-Pactil, A.M. Bondzic, V. Vasic, *Pharmacol. Toxicol. Cur. Neuropharmacol.* 11 (2013) 315-335. DOI: 10.2174/1570159X11311030006
- [15] M. Atanasova, G. Stavrakov, L. Philipova, D. Zheleva, N. Yordanov, I. Doytchinova, *Bioorg. Med. Chem.* 23 (2015) 5382-5389. DOI: 10.1016/j.bmc.2015.07.058
- [16] D. Genest, C. Rochais, C. Lecoutey, S. Jana Sopkova-de Oliveira, C. Ballandonne, S. Butt-Gueulle, R. Legay, M. Since, P. Dallemagne, *Med. Chem. Commun.* 4 (2013) 925-931. DOI: 10.1039/C3MD00041A
- [17] Z.F. Al-Rashid, R.P. Hsung, *Bioorg. Med. Chem.* 25 (2015) 4848-4853. DOI: 10.1016/j.bmcl.2015.06.047
- [18] M. Alipour, M. Khoobi, A. Foroumadi, H. Nadri, A. Moradi, A. Sakhteman, M. Ghandi, A. Shafiee, *Bioorg. Med. Chem.* 20 (2012) 7214-7222. DOI: 10.1016/j.bmc.2012.08.052
- [19] J. Cheung, M.J. Rudolph, F. Burshteyn, M.S. Cassidy, E.N. Gary, J. Love, C.F. Matthew, J.J. Height, *J. Med. Chem.* 55 (2012) 10282-10286. DOI: 10.1021/jm300871x
- [20] W. Huang, H. Yu, R. Sheng, J. Li, Y. Hu, *Bioorg. Med. Chem.* 16 (2008) 10190-10197. DOI: 10.1016/j.bmc.2008.10.059
- [21] R. Sheng, X. Lin, J. Li, Y. Jiang, Z. Shang, Y. Hu, *Bioorg. Med. Chem. Lett.* 15 (2005) 3834-3837. DOI: 10.1016/j.bmcl.2005.05.132
- [22] R. Leurs, R.A. Bakker, H. Timmerman, I. de Esch, *J. Nat. Rev. Drug Discov.* 4 (2005) 107-120. DOI:10.1038/nrd1631
- [23] B. N. Saglik, S. Ilgin, Y. Ozkay, *Eur. J. Med. Chem.* 124 (2016) 1026-1040. DOI: 10.1016/j.ejmech.2016
- [24] L. Hong, R. T. Turner, G. Koelsch, D. Shin, A. K. Ghosh, J. Tang, *Biochemistry* 41 (2002) 10963-10967. DOI: 10.1021/bi026232n
- [25] F. Prati, G. Bottegoni, M. L. Bolognesi, A. Cavalli, *J. Med. Chem.* 61 (2018) 619-637. DOI: 10.1021/acs.jmedchem.7b00393
- [26] N. Y. Mok, J. Chadwick, K. A. B. Kellett, N. M. Hooper, A. P. Johnson, C. W. G. Fishwick, *Bioorg. Med. Chem.* 19 (2009) 6770-6774. DOI: 10.1016/j.bmcl.2009.09.103
- [27] X. Zhao, D. Gong, Y. Jiang, D. Guo, Y. Zhu, Y. Deng, *Eur. J. Med. Chem.* 138 (2017) 738-747. DOI: 10.1016/j.ejmech.2017.07.006
- [28] L. Piazzzi, A. Cavalli, F. Colizzi, F. Belluti, M. Bartolini, F. Mancini, M. Recanatini, V. Andrisano, A. Rampa, *Bioorg. Med. Chem. Lett.* 18 (2008) 423-426. DOI:10.1016/j.bmcl.2007.09.100
- [29] P. Costanzo, L. Cariati, D. Desiderio, R. Sgammato, A. Lamberti, R. Arcone, R. Salerno, M. Nardi, M. Masullo, M. Oliverio, *ACS Med. Chem. Lett.* 7 (2016) 470-475. DOI: 10.1021/acsmedchemlett.5b00483
- [30] J. Yuan, S. Venkatraman, Y. Zheng, B. M. McKeever, L. W. Dillard, B. S. Singh, *J. Med. Chem.* 56 (2013) 4156-4180. DOI: 10.1021/jm301659n
- [31] M. I. Fernandez-Bachiller, C. Perez, L. Monjas, J. Rademann, M. I. Rodriguez-Franco, *J. Med. Chem.* 55 (2012) 1303-1317. DOI: 10.1021/jm201460y
- [32] F. Li, Z.-M. Wang, J.-J. Wu, J. Wang, S.-S. Xie, J.-S. Lan, W. Xu, L.-Y. Kong, X.-B. Wang, *J. Enzyme Inhib. Med. Chem.* 31 (2016) 41-53. DOI:10.1080/14756366.2016.1201814
- [33] W. Xu, X.-B. Wang, Z.-M. Wang, J.-J. Wu, F. Li, J. Wang, L.-Y. Kong, *Med. Chem. Commun.* 7 (2016) 990-998. DOI: 10.1039/C6MD00053C
- [34] L. Di, E. H. Kerns, K. Fan, O. J. McConnell, G. T. Carter. *Eur. J. Med. Chem.* 38 (2003) 223-232. DOI: [https://doi.org/10.1016/S0223-5234\(03\)00012-6](https://doi.org/10.1016/S0223-5234(03)00012-6)

- [35] L. Di, E. H. Kerns. *Curr. Opin. Chem. Biol.* 7 (2003) 402-408. DOI: [https://doi.org/10.1016/S1367-5931\(03\)00055-3](https://doi.org/10.1016/S1367-5931(03)00055-3)
- [36] S. Pfaender, A. M. Grabrucker, *Metallomics*, 6 (2014) 960-977. DOI: 10.1039/c4mt00008k
- [37] J. A. Duce, A. I. Bush, *Prog. Neurobiol.* 92 (2010) 1-18. DOI: 10.1016/j.pneurobio.2010.04.003
- [38] A. Budimir, *Acta Pharm.* 61 (2011) 1-14. DOI:10.2478/v10007-011-0006-6
- [39] C. Lu, Y. Guo, J. Yan, Z. Luo, H.-B. Luo, M. Yan, L. Huang, X. Li, *J. Med. Chem.* 56 (2013) 5843-5859. DOI: 10.1021/jm400567s
- [40] M. P. Cuajungco, K. Y. Faget, X. Huang, R. E. Tanzi, A. I. Bush, *Ann. N. Y. Acad. Sci.* 920 (2000) 292-304. DOI: <https://doi.org/10.1111/j.1749-6632.2000.tb06938.x>
- [41] G. Liu, M. R. Garrett, P. Men, X. Zhu, G. Perry, M. A. Smith, *Biochim. Biophys. Acta, Mol. Basis Dis.*, 1741 (2005) 246-252. DOI: 10.1016/j.bbadis.2005.06.006
- [42] G. L. Ellman, K. D. Courtney, V. Andres, R. M. Feather-Stone, *Biochem. Pharmacol.* 7 (1961) 88-90. DOI: [https://doi.org/10.1016/0006-2952\(61\)90145-9](https://doi.org/10.1016/0006-2952(61)90145-9)
- [43] M. E. Kennedy, W. Wang, L. Song, J. Lee, L. Zhang, G. Wong, L. Wang, E. Parker. *Anal. Biochem.* 319 (2003) 49-55. DOI: [https://doi.org/10.1016/S0003-2697\(03\)00253-7](https://doi.org/10.1016/S0003-2697(03)00253-7)
- [44] F. Mancini, A. De Simone, V. Andrisano. *Anal. Bioanal. Chem.* 400 (2011) 1979-1996. DOI: 10.1007/s00216-011-4963-x
- [45] T. Mosmann, *J. Immunol. Methods* 65 (1983) 55-63. DOI: [https://doi.org/10.1016/0022-1759\(83\)90303-4](https://doi.org/10.1016/0022-1759(83)90303-4)
- [46] F. Denizot, R. Lang, *J. Immunol. Methods* 89 (1986) 271-277. DOI: [https://doi.org/10.1016/0022-1759\(86\)90368-6](https://doi.org/10.1016/0022-1759(86)90368-6)
- [47] D. Gerlier, T. Thomasset, *J. Immunol. Methods* 94 (1986) 57-63. DOI: [https://doi.org/10.1016/0022-1759\(86\)90215-2](https://doi.org/10.1016/0022-1759(86)90215-2)

Highlights

- Donepezil analogues as multi-target-directed ligands
- Dual inhibition of AChE and BACE-1 in the nanomolar range
- Molecular modeling reveals dual mechanism against AChE and BACE-1
- Compound **4** shows potential biometal chelation ability and high BBB permeability

Graphical abstract

Profiling donepezil template to dual AChE and BACE-1 inhibition

